J. Univ. Kuwait (Sci.) **21**, 1994

Active control of nonlinear vibrations in cable stayed bridges by tendons

MOHAMED ABDEL-ROHMAN AND HASAN ASKAR

Department of Civil Engineering, Kuwait University, P.O. Box 5969, 13060 Safat, Kuwait

ABSTRACT

This paper shows the active control of nonlinear vibration in cable stayed bridges using a tendon mechanism and investigates the effect of neglecting high order modes in the design of the control law on the controlled response. The paper finds out that many vibrational modes should be considered in the design of the velocity feedback control law, in order to obtain a stable and damped controlled response as designed.

INTRODUCTION

Cable stayed bridges are large flexible structures susceptible to dynamic loading actions such as wind forces. The flexibility of such structures generates self-excited forces due to source-structure interaction, which make the structure behave in a non-linear manner. Several control mechanisms, including passive and active controls, have been devised to control the response of large flexible structures, such as cable stayed bridges.

In a previous comprehensive study, by the first author and others the use of passive tuned mass damper (PTMD) control mechanism to control the response of cable stayed bridges has fallen short of providing enough damping percentage to the typical cable stayed bridge. The active TMD control mechanism has shown the ability to reduce the response of the bridge by introducing enough active damping percentage, providing that the active control force should be properly designed.

This paper shows the control of the cable stayed bridge using active tendon control mechanism. This mechanism can be formed using some of the cables in the bridge to generate the active control forces. One may connect the cables to the bridge deck by hydraulic actuators which are automatically operated according to the designed control law (Abdel-Rohman 1984, Abdel-Rohman & Nayfeh 1987, Chung *et al.* 1988, Hart & Yao 1977, Miller *et al.* 1988, Reinhorn *et al.* 1987, Soong 1988, Yao and Abdel-Rohman 1985).

Most of the previous applications on using active tendon control mechanisms focused on the response of the first bending fundamental. In this paper the controlled response of the first bending made the first three bending modes of the bridge using a tendon control mechanism will be shown. From this investigation the effect of neglecting high order modes in the design of the control law on the controlled response is shown.

EQUATION OF MOTION

Figure 1 shows the cable stayed bridge, considered in this paper, and the elevations and dimensions, while the finite elements discretization of the bridge is shown in Figs. 2 and 3. Tables 1 and 2 give the ordinates of the first and third bending mode shapes at every element nodes, resulting from using M-SAP finite element program. The second mode is antisymmetric and does not contribute into the response at mid-span. Figure 4 shows a tendon control mechanism in which two cables are connected at mid-span of the bridge with the two towers of the bridge.

The equation of motion of the first bending mode can be expressed as

$$\ddot{A}_1 + 2\xi_1\omega_1\dot{A}_1 + \omega_1^2 A_1 = F_1 - \frac{a_1^T}{M_1}U \tag{1}$$

in which $A_1(t)$ is the time response of the first mode; ω_1, ξ_1 are respectively, the natural frequency and damping ratio of the first mode obtained from the finite

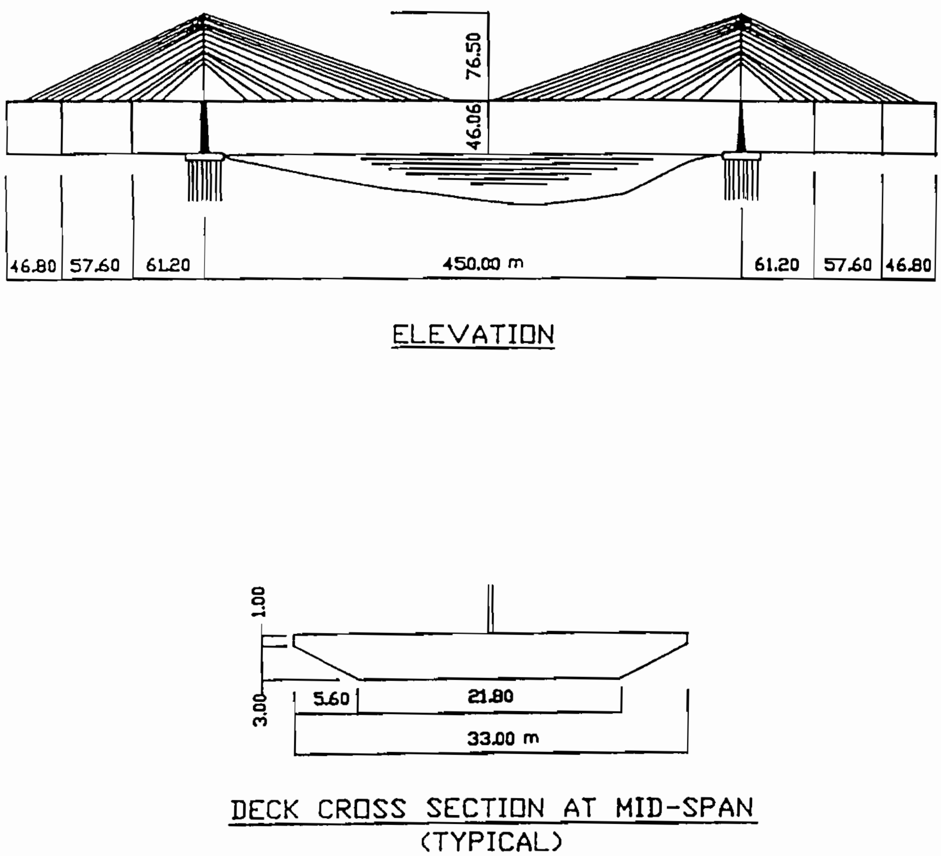

Fig. 1.

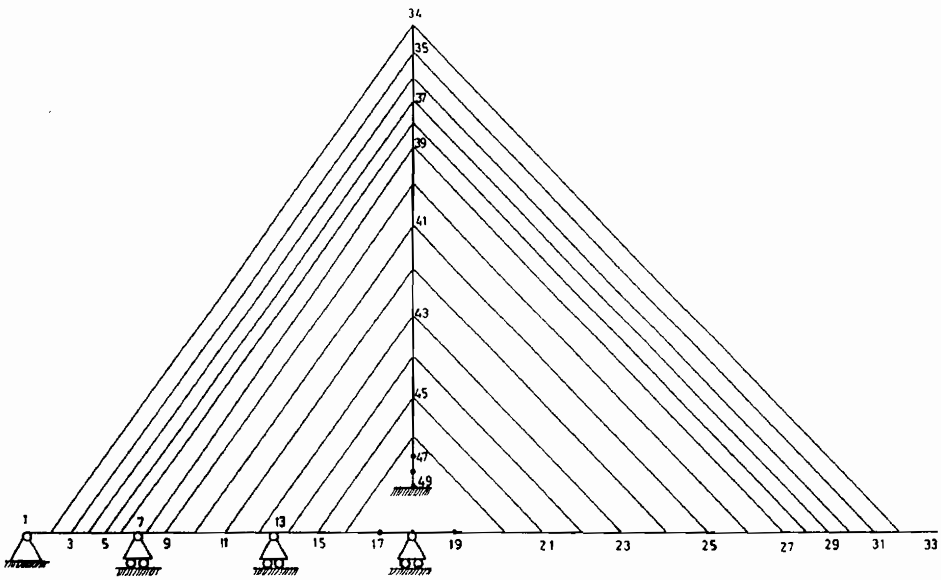

Fig. 2. Joint Coordinates.

element program. The first modal mass M_1 is estimated from the mode shape $\boldsymbol{a}_1$ which is a scaled mode shape from the normalized first mode shape ϕ_1 at any node j. The first modal mass is $M_1 = (a_{1j}/\phi_{1j})^2$. The active control forces vector $\boldsymbol{U}$ are obtained from operating the hydraulic actuators, which pull or release the cables according to a designed control law. The wind force at node j is expressed as (Simiu &

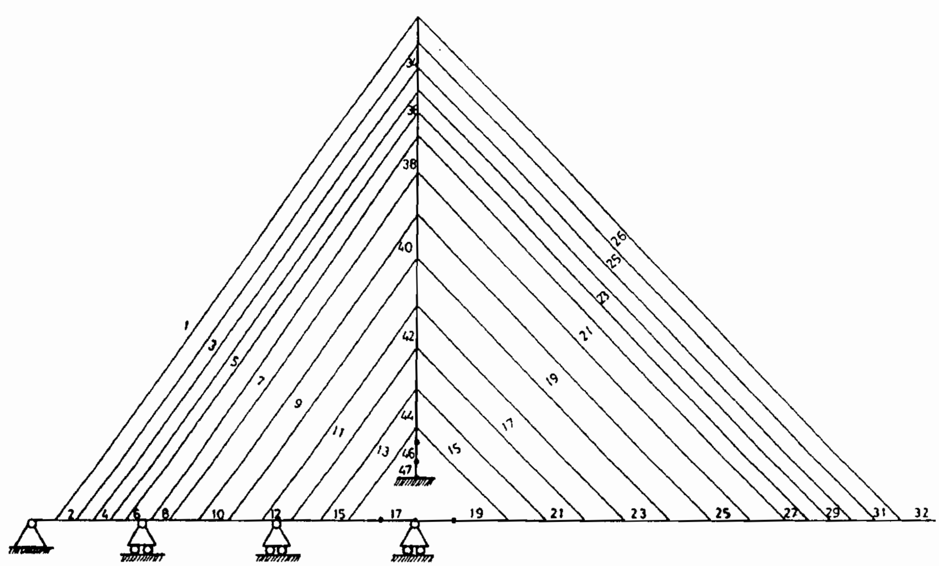

Fig. 3. Member Incidences.

Table 1. First mode shape.

Joint	ϕ_1	a_1	Joint	ϕ_1	a_1
1	0	0	25	−0.012 E-1	+0.4517
2	0.13 E-3	−0.0057	26	−0.137 E-1	+0.6008
3	0.148 E-3	−0.0065	27	−0.163 E-1	+0.7149
4	0.126 E-3	−0.0055	28	−0.179 E-1	+0.7851
5	0.743 E-3	−0.0032	29	−0.194 E-1	+0.8508
6	0.183 E-3	−0.0008	30	−0.206 E-1	+0.9035
7	0.000	0.000	31	−0.216 E-1	+0.9473
8	−0.199 E-5	+0.000087	32	−0.224 E-1	+0.9824
9	0.342 E-4	−0.0015	33	−0.228 E-1	+1.0000
10	0.707 E-4	−0.0031	34	+0.377 E-2	−0.1653
11	0.34 E-4	−0.0015	35	0.357 E-2	−0.1565
12	−0.142 E-5	+0.00006	36	0.337 E-2	−0.1478
13	0.000	0.000	37	0.317 E-2	−0.13904
14	0.148 E-4	−0.00065	38	0.297 E-2	−0.1303
15	0.977 E-4	−0.0043	39	0.277 E-2	−0.1215
16	0.18 E-4	−0.0078	40	0.247 E-2	−0.1083
17	0.2057 E-3	−0.009	41	0.029 E-2	−0.0916
18	0.000	0.000	42	0.173 E-2	−0.0758
19	−0.512 E-3	+0.0224	43	0.147 E-2	−0.0644
20	−0.138 E-2	+0.0605	44	0.132 E-2	−0.0578
21	−0.25 E-2	+0.1096	45	0.110 E-2	−0.0482
22	−0.398 E-2	+0.1745	46	0.901 E-3	−0.0395
23	−0.516 E-2	+0.2263	47	0.310 E-3	−0.2136
24	−0.719 E-2	+0.3153	48	0.395 E-4	−0.0017

Table 2. Third mode shape.

Joint	ϕ_3	a_3	Joint	ϕ_3	a_3
1	0.0	0.0	25	−0.17815 E-1	−1.04017
2	−0.19062 E-4	−0.00111297	26	−0.11550 E-1	−0.6743737
3	−0.19087 E-4	−0.001114439	27	−0.4823 E-2	−0.283896
4	−0.12978 E-4	−7.5775 E-4	28	0.25955 E-4	0.00151544
5	−0.49605 E-5	−2.8963 E-4	29	0.48581 E-2	0.283651
6	−0.70048 E-7	−4.0899 E-6	30	0.92775 E-2	0.5416885619
7	0.0	0.0	31	0.12947 E-1	0.7559409
8	−0.10195 E-5	−5.9525 E-5	32	0.15577 E-1	0.909499
9	−0.26935 E-4	−0.00157266	33	0.17127 E-1	1.0
10	−0.12715 E-3	−0.0074239	34	−0.11816 E-2	−0.6899
11	−0.21310 E-3	−0.0124365	35	−0.65251 E-3	−0.038098
12	−0.10572 E-3	−0.0061727	36	−0.12542 E-3	−0.0073229
13	0.0	0.0	37	0.39161 E-3	0.022865
14	0.15650 E-3	0.009137618	38	0.89239 E-3	0.0521036
15	0.76928 E-3	0.04491621	39	0.13646 E-2	0.07967536
16	0.13349 E-2	0.0779413	40	0.1980 E-2	0.1156069
17	0.15052 E-2	0.08788462	41	0.26185 E-2	0.1528872
18	0.0	0.0	42	0.30127 E-2	0.175903
19	−0.35766 E-2	−0.2088281	43	0.31325 E-2	0.1828983
20	−0.83415 E-2	−0.4870380	44	0.31333 E-2	0.182945
21	−0.12854 E-1	−0.75051	45	0.30300 E-2	0.1769136
22	−0.16814 E-1	−0.9817247	46	0.28091 E-2	0.16401588
23	−0.18717 E-1	−1.092935	47	0.13757 E-2	0.080323
24	−0.19914 E-1	−1.1627255	48	0.21188 E-3	0.0123711
			49	0.0	0.0

Scanlan 1986)

$$F_j = \tfrac{1}{2}\rho V^2 (2B) H^* \left[1 - \epsilon \frac{Y_j^2}{B^2}\right] \frac{\dot{Y}_j}{V} \Delta X_j \tag{2}$$

in which ρ = air density, V = mean wind speed m/sec., B = bridge width in meter, Y_j is vertical deflection at j in meter, $\dot{Y}_j$ is vertical velocity at j, H^* and ϵ are constants from wind data given as $H^* = 14.06/M_1\ \text{sec}^3$ and $\epsilon = 237\,000$ (Malhotra, 1987).

Equation (2) can be expressed, considering Y is given by the first bending mode only, as

$$F_j = \rho V B H^* \left[1 - \epsilon \frac{\phi_{1j}^2 A_1^2}{B^2}\right] \phi_{1j} \dot{A}_1 \Delta X_j \tag{3}$$

Considering Eqn (3) which is valid for one mode only, the generalized wind force on the first mode is obtained from

$$F_1 = \rho V B H^* \left[\sum_j \phi_{1j}^2 \Delta X_j - \frac{\epsilon}{B^2} A_1^2 \sum_j \phi_{1j}^4 \Delta X_j\right] \dot{A}_1 \tag{4}$$

The active control force vector $\boldsymbol{U}$ is a zero vector except at the tower and midspan nodes where the active forces are applied. Given the numbering scheme shown in Fig. 2, the vector $\boldsymbol{U}$ contains zeros except at elements (33) and (34) where the active control force equals $(2U \sin\theta)$ and $(2U \cos\theta)$, respectively, i.e.

$$\boldsymbol{U}^T = [0\ 0\ 0\ 0\ 0 \ldots \underset{(33)}{(2U \sin\theta)}\ \ \underset{(34)}{(2U\cos\theta)}\ 0\ 0 \ldots 0]_{1\times 49} \tag{5}$$

where the angle θ is 18.7° as shown in Fig. 4.

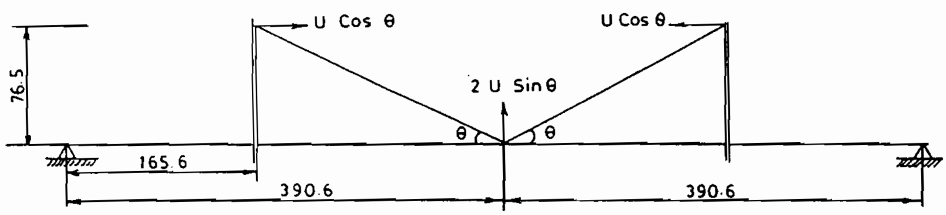

Fig. 4.

The first bending mode equation becomes

$$\ddot{A}_1 + 2\xi_1\omega_1\dot{A}_1 + \omega_1^2 A_1 = 1.5376\dot{A}_1 - 0.12268\dot{A}_1 A_1^2 - 1.72285 \times 10^{-4} U(t) \tag{6}$$

ACTIVE CONTROL USING VELOCITY FEEDBACK

The control force $U(t)$ can be operated proportional to the velocity response at midspan (Abdel-Rohman & Leipholz 1978). The control law is expressed as follows:

$$U(t) = \bar{\alpha}\dot{y}_{m.s.} = \bar{\alpha} \sum_i \phi_{1m.s.} \dot{A}_i \tag{7}$$

in which $\bar{\alpha}$ is a constant.

For the purpose of design, the contribution of one mode only is considered. Equation 7 can be written as

$$\begin{aligned} U(t) &= \bar{\alpha}\phi_{1m.s.}\dot{A}_1 \\ &= \alpha\dot{A}_1 \end{aligned} \tag{8}$$

where $\phi_{1m.s.} = 0.0228$, and $\alpha = 0.0228\bar{\alpha}$, which shall be determined. Substituting Eqn. 8 into Eqn. 6 one obtains the equation of the controlled response considering the first bending mode. The value of α is determined according to the magnitude of damping required. For $\xi\%$ damping ratio the value of α is obtained from the following equation:

$$2\xi_1\omega_1 + 1.72285 \times 10^{-4}\alpha = 2 \times \xi \times \omega_1 \tag{9}$$

For 20% damping ratio α is obtained to be 4389.24, and for 30% damping ratio α is 6699.4. The controlled response of the phase plane using the above active damping ratios are shown in Figs. 5 and 6 which are obtained from the numerical integration of Eqn. 6. These figures are compared with the uncontrolled response shown in Fig. 7.

EQUATIONS OF MOTION OF TWO MODES

In order to check the effectiveness of the velocity feedback control law designed for one mode response only, the response due to the first and third bending modes is considered. The second mode is symmetric and does not contribute to the deflection

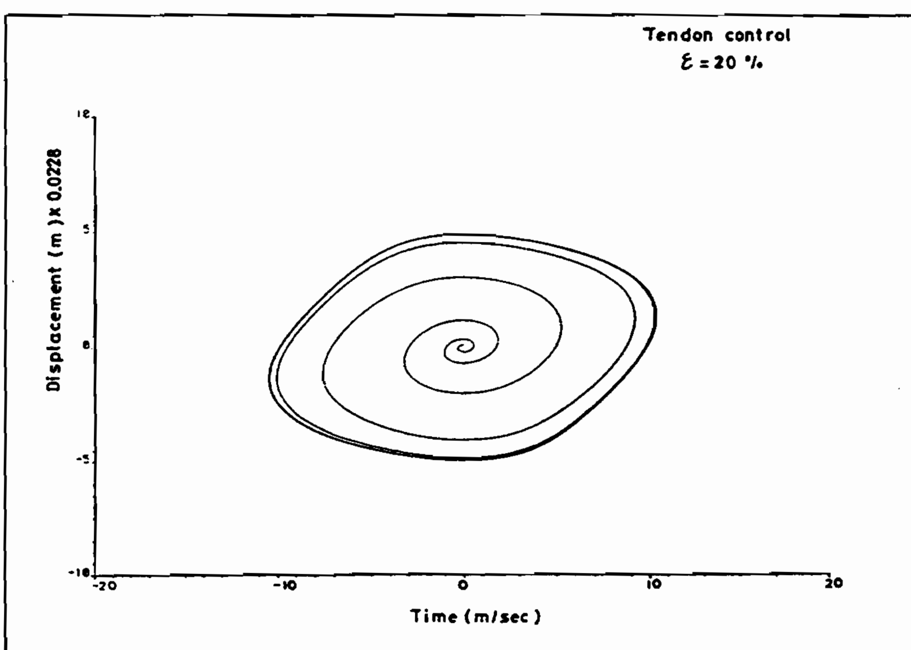

Fig. 5.

at mid-span. The equations of motion for the two modes become

$$\ddot{A}_1 + 2\xi_1\omega_1\dot{A}_1 + \omega_1^2 A_1 = \phi_1^T \boldsymbol{F} \tag{10}$$

$$\ddot{A}_3 + 2\xi_3\omega_3\dot{A}_3 + \omega_3^2 A_3 = \phi_3^T \boldsymbol{F} \tag{11}$$

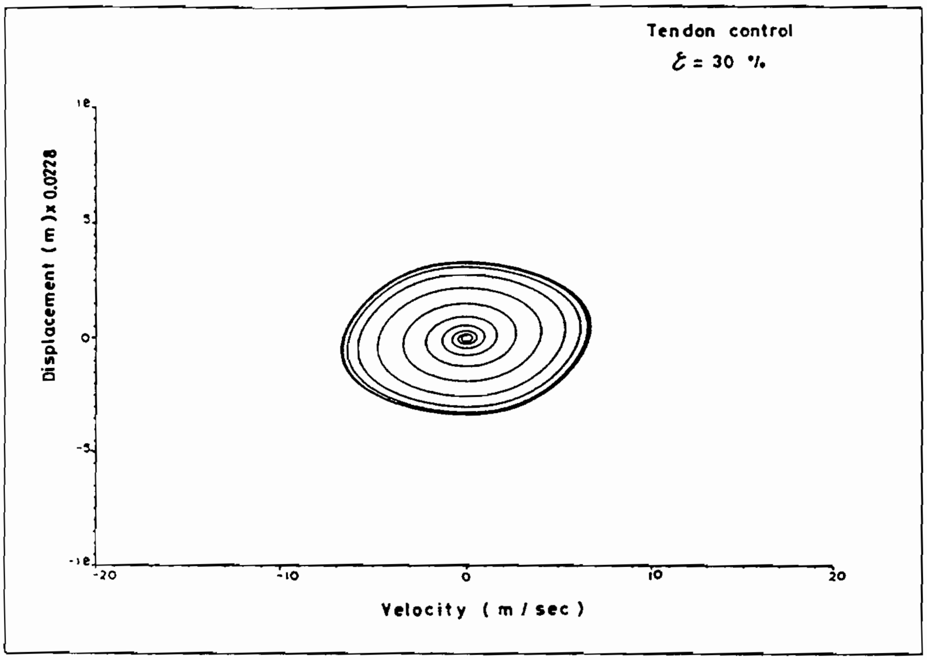

Fig. 6.

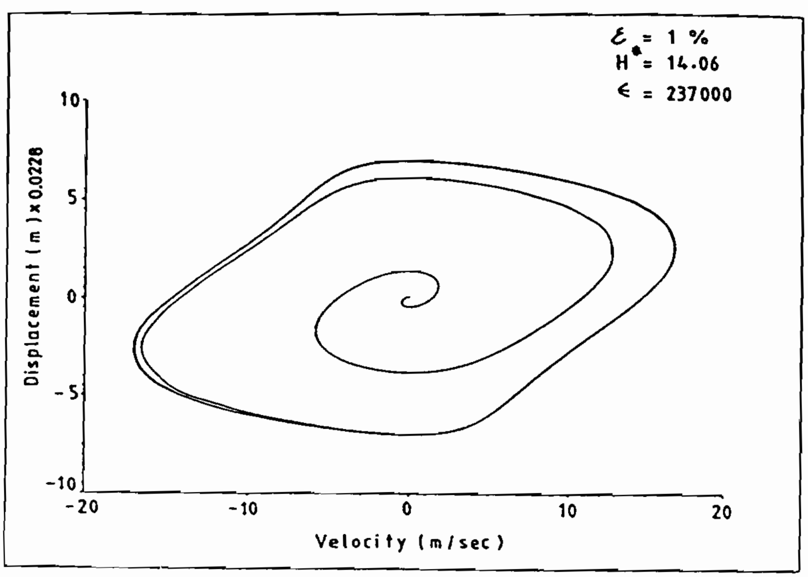

Fig. 7.

in which F is the nodal wind force vector estimated using the formula

$$F_j = \rho V^2 BH^* \left[1 - \frac{\epsilon}{B^2}(\phi_{1j}A_1 + \phi_{3j}A_3)^2\right](\phi_{1j}\dot{A}_1 + \phi_{3j}\dot{A}_3)\frac{\Delta X_j}{V} \tag{12}$$

The first and third bending modes contribute to the deflection at mid-span ($\omega_1 = 1.99$ and $\omega_3 = 4.236$). Carrying out the calculations on the right hand side of Eqns. 10 and 11 using Eqn. 12 and using the mode shapes listed in Tables 1 and 2 one obtains

$$\begin{aligned}\phi_1^T F = {} & 1.53757\dot{A}_1 - 0.00425\dot{A}_3 - 0.12266\dot{A}_1 A_1^2 \\ & + 0.08846 A_1\dot{A}_1 A_3 - 0.42228\dot{A}_1 A_3^2 + 0.04423 A_1^2\dot{A}_3 \\ & - 0.103312 A_1 A_3\dot{A}_3 - 0.006708 A_3^2\dot{A}_3\end{aligned} \tag{13}$$

$$\begin{aligned}\phi_3^T F = {} & -0.005096\dot{A}_1 + 1.80792\dot{A}_3 + 0.05297\dot{A}_1 A_1^2 \\ & - 0.123732 A_1\dot{A}_1 A_3 - 0.008\dot{A}_1 A_3^2 - 0.06186 A_1^2\dot{A}_3 \\ & - 0.001345 A_1 A_2\dot{A}_2 - 0.1076685 A_2^2\dot{A}_2\end{aligned} \tag{14}$$

The uncontrolled response expressed in terms of the phase plane is shown in Fig. 8. In order to investigate the controlled response considering the first three modes, the active control force $U(t)$ is expressed as in Eqn. 7 by

$$U(t) = \bar{\alpha}(\phi_{1m.s.}\dot{A}_1 + \phi_{3m.s.}\dot{A}_3) \tag{15}$$

where $\phi_{1m.s.} = 0.0228\phi_{3m.s.} = -0.01712$, and $\bar{\alpha}$ is the same as determined when dealing with one mode only.

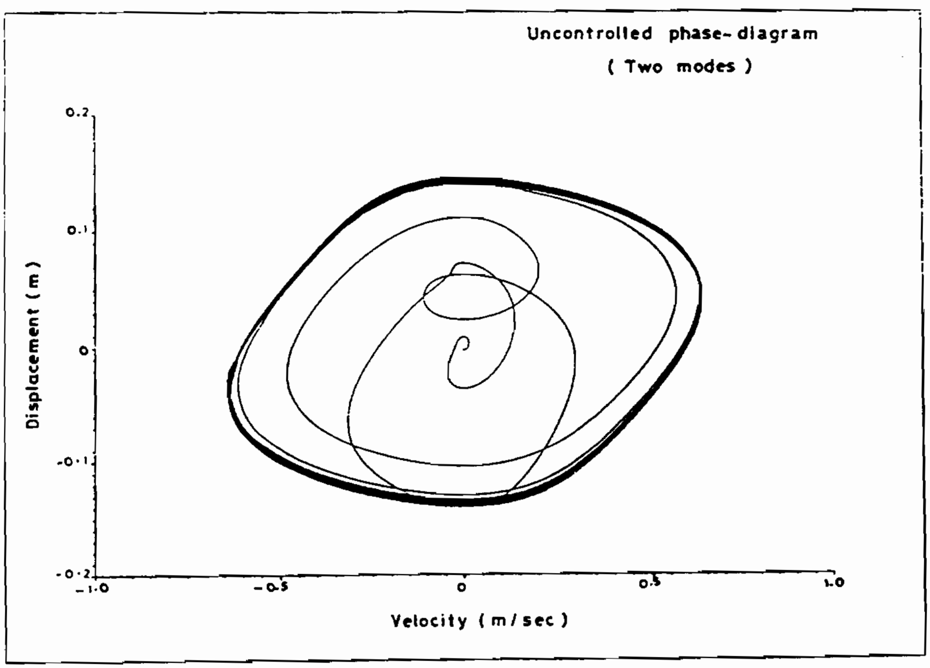

Fig. 8.

The equations of motion of the first and third controlled modes are

$$\ddot{A}_1 + 2\xi_1\omega_1\dot{A}_1 + \omega_1^2 A_1 = \phi_1^T F - \frac{a_1^T}{M_1} U$$

$$\ddot{A}_3 + 2\xi_3\omega_3\dot{A}_3 + \omega_3^2 A_3 = \phi_3^T F - \frac{a_3^T}{M_3} U \tag{16}$$

in which $M_1 = \phi_{1m.s.}^{-2} = 1917.944$ and $M_3 = \phi_{3m.s.}^{-2} = 3409.08$.

Substituting Eqns. 13 to 15 into Eqn. 16, one obtains the equations of motion of the controlled response. The controlled response at mid span for the phase plane using the same values of α determined previously when considering one mode only are shown in Figs. 9 and 10. One observes that for 20% damping ratio, the steady state deflection considering one mode as shown in Fig. 5 is $(5 \times \phi_{1m.s.}) = 0.114$ ft. For the first three modes, the steady state deflection at mid span is shown in Fig. 9 to be 0.1 ft, which is very close. For comparison of deflection and velocity responses, at mid-span, the following indices are used, respectively,

$$J_D = \int_0^T (\phi_1 A_1 + \phi_3 A_3)^2 \, dt \tag{17}$$

$$J_V = \int_0^T (\phi_1 \dot{A}_1 + \phi_3 \dot{A}_3)^2 \, dt \tag{18}$$

in which T is an arbitrary time period.

Comparison between the response of one and three modes for the controlled and uncontrolled structures is shown in Figs. 11–14. It is concluded that the difference

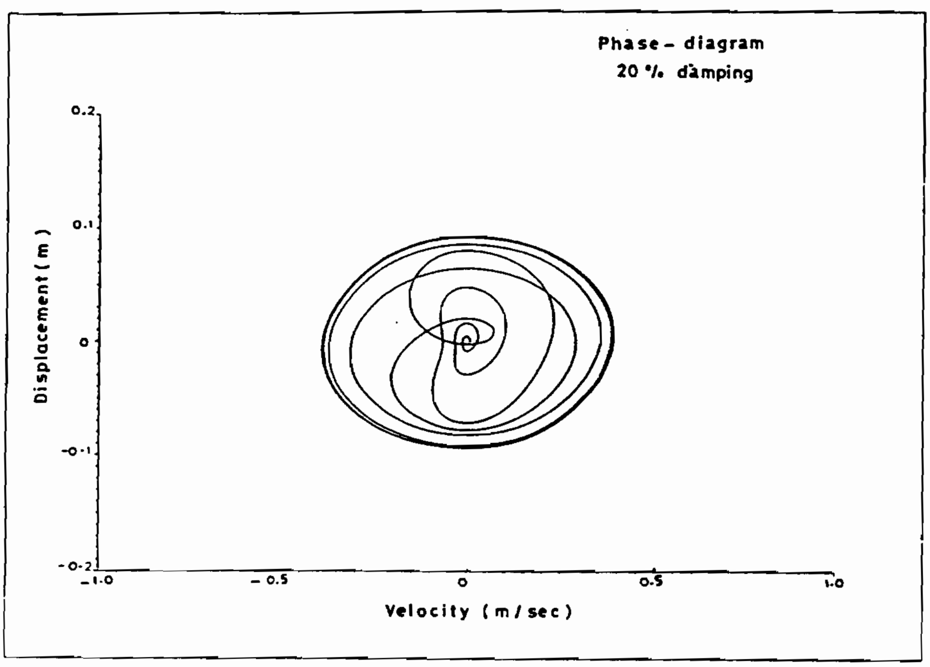

Fig. 9.

between the uncontrolled response and the controlled response considering one mode is much higher than the difference when considering three modes. It is therefore recommended to design the velocity feedback control law considering as many modes as possible in order to guarantee a stable controlled response as designed.

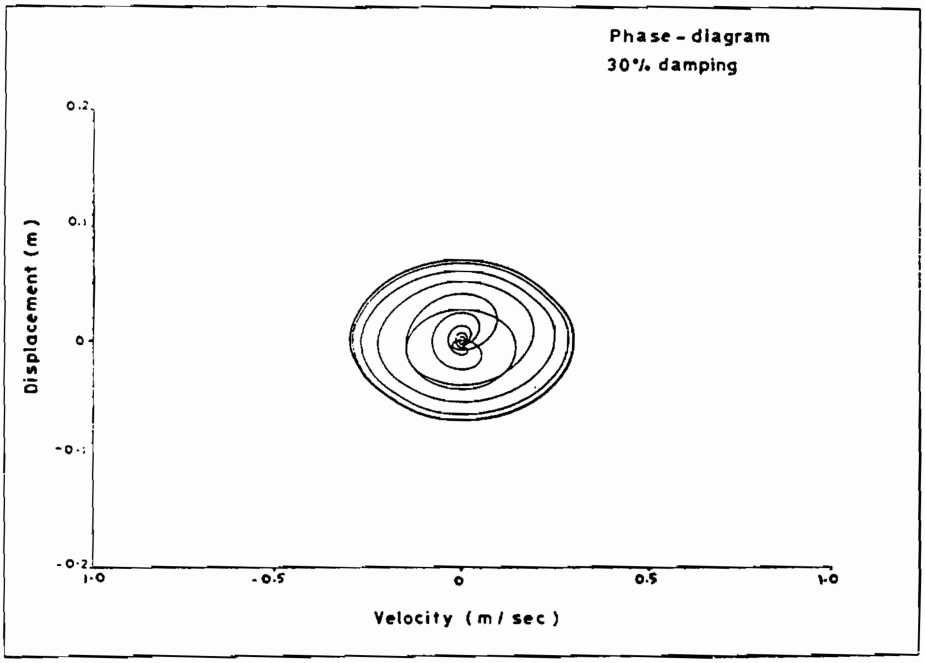

Fig. 10.

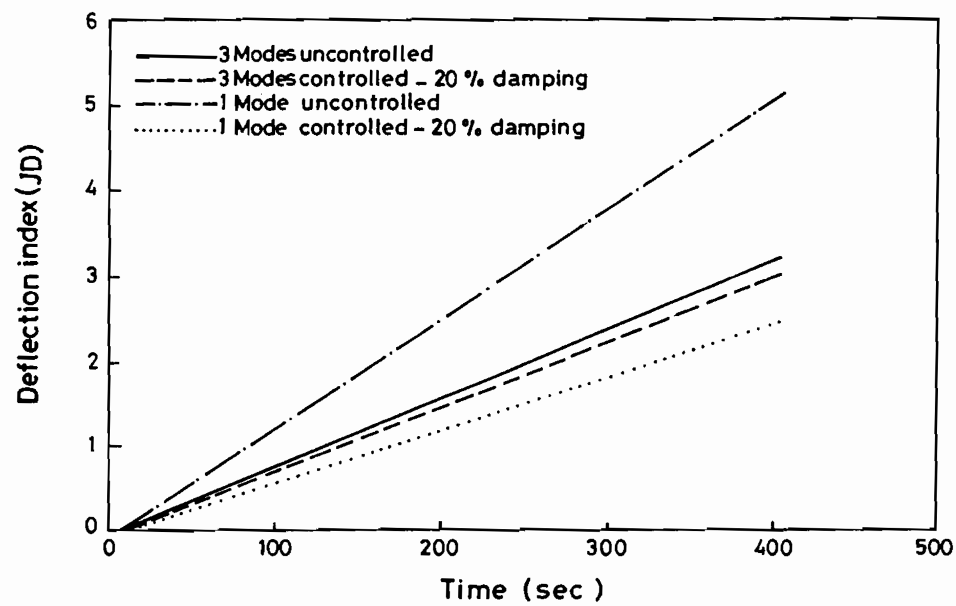

Fig. 11.

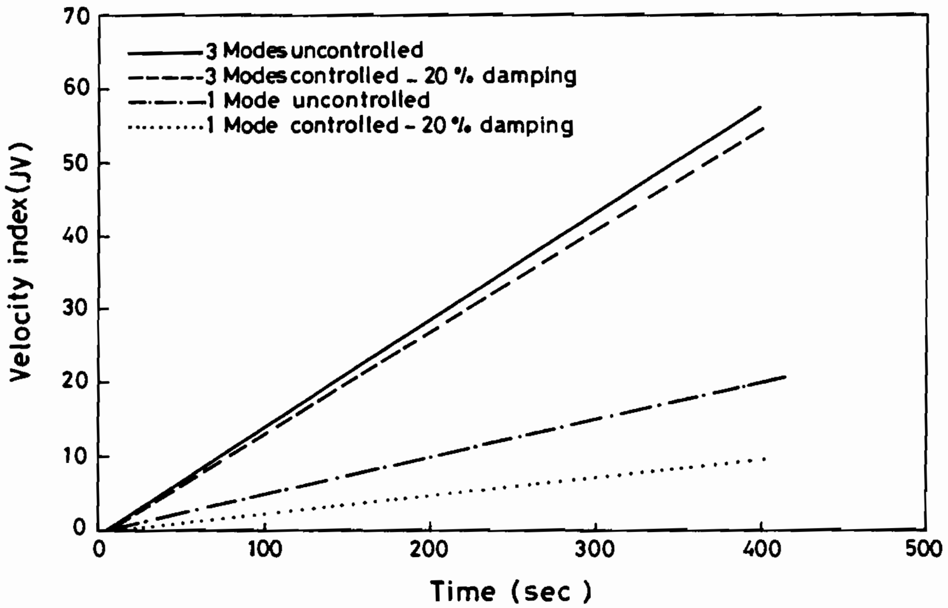

Fig. 12.

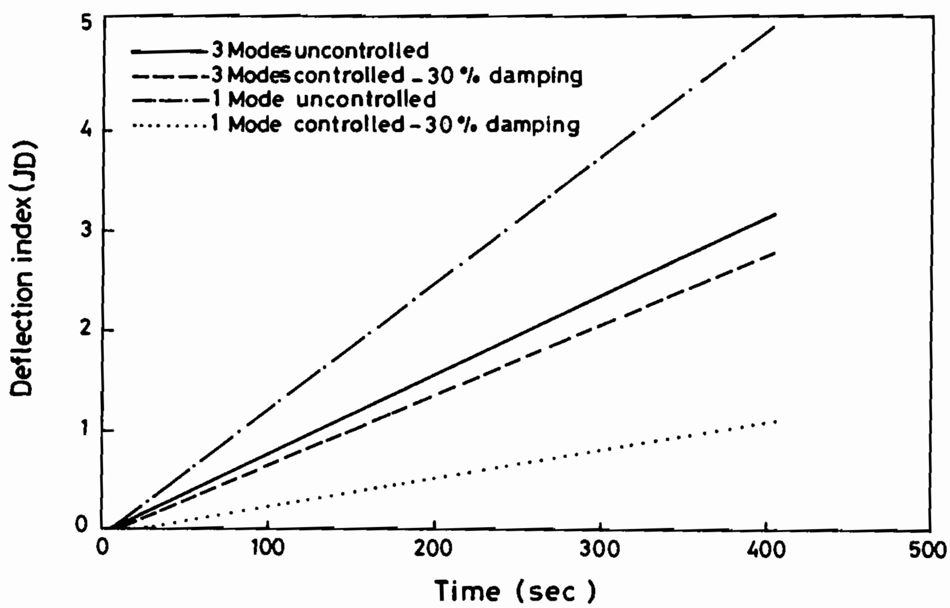

Fig. 13.

CONCLUSIONS

This paper has shown that the design of a velocity feedback control law based on a small number of the first bending modes may deceive the designer when it gives good controlled response. In reality, the high order modes may minimize the gained benefit from the control or even may destabilize the controlled response. Therefore, it is recommended to consider as many modes as possible in the design of the velocity feedback control law in order to minimize the spillover effect of the higher order modes. One can suffice with the number of modes when he finds that including higher order modes does not, significantly, change the controlled response.

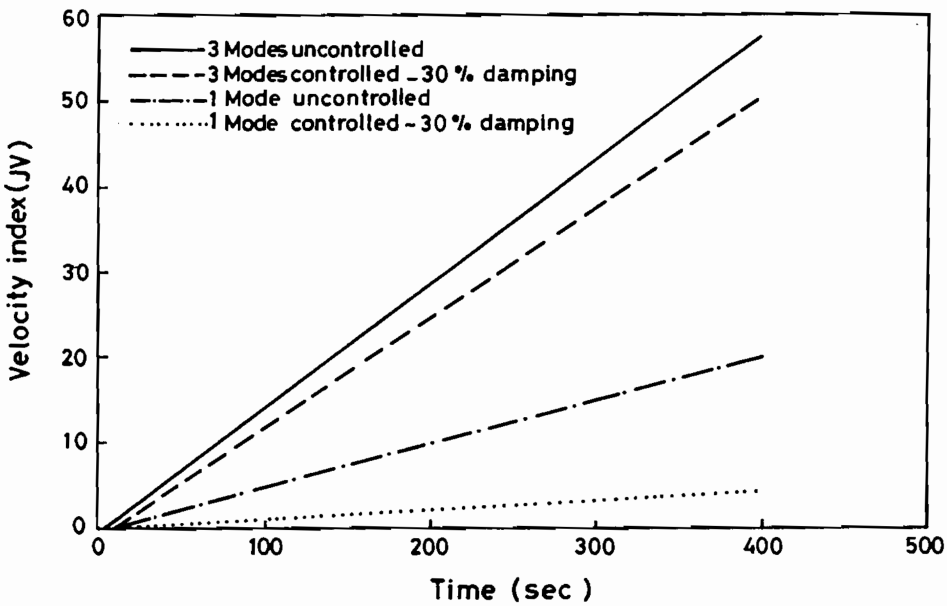

Fig. 14.

ACKNOWLEDGEMENT

The research of this paper was supported by the research unit under grant EV038.

REFERENCES

Abdel-Rohman, M. 1984. Active control of tall buildings against stochastic wind forces. Journal of Wind Engineering and Industrial Aerodynamics **17:** 251-64.

Abdel-Rohman, M. & Leipholz, H. 1978. Structural control by the pole assignment method. Journal of Engineering Mechanics, ASCE **104:** 1159–75.

Abdel-Rohman, M. & Nayfeh, A. 1987. Passive control of nonlinear oscillations in bridges. Journal of Engineering Mechanics, ASCE **113(11):** 1694–708.

Chung, L.L., Reinhorn, A.M. & Soong, T.T. 1988. Experiments on active control of seismic structures. Journal of Engineering Mechanics, ASCE **114(2):** 241–56.

Malhotra, P.K. 1987. Tuned mass damper for suppressing wind effects in cable-stayed bridge decks. M.Sc. thesis, AIT, Bangkok, Thailand.

Miller, R.K., Masri, S.F., Dehghauyar, T.J. & Caughey, T.K. 1988. Active vibration control of large civil structures. Journal of Engineering Mechanics, ASCE **114(9):** 1542–71.

Reinhorn, A.M., Manolis, G.D. & Wen, C.Y. 1987. Active control of inelastic structures. Journal of Engineering Mechanics, ASCE **113(3):** 315–33.

Simu, E. & Scanlan, R.H. 1986. Wind effects on structures. J. Wiley, N.Y.

Soong, T.T. 1988. Active structural control in civil structures: State of the art review. Journal of Engineering Structures **10(2):** 74–84.

Yao, J.T.P. & Abdel-Rohman, M. 1985. Research topics for practical implementation of structural control. 2nd Symposium on Structural Control, North Holland: 762–7.

(Received 15 May 1993, revised 22 January 1994)

التحكم الفعال في الأهتزازات اللاخطية في الجسور المعلقة بإستخدام الكابلات

محمد عبدالرحمن وحسن عسكر
قسم الهندسة المدنية، بجامعة الكويت،
ص. ب ٥٩٦٩، الصفاة ١٣٠٦٠، الكويت

خلاصة

هذا البحث يبين كيفية التحكم الفعال في الأهتزازات اللاخطية في الجسور المعلقة بإستخدام الكابلات ويدرس تأثير إهمال نماذج الأهتزازات العالية في تصميم قانون التحكم على السلوك بعد إدخال التحكم الفعال.

يستخلص البحث إنه يجب الأخذ في الأعتبار أكبر عدد ممكن من نماذج الأهتزازات في تصميم قانون التحكم لضمان أمان سلوك المنشأ بعد التحكم.